

TWO-WEEK LOAN COPY

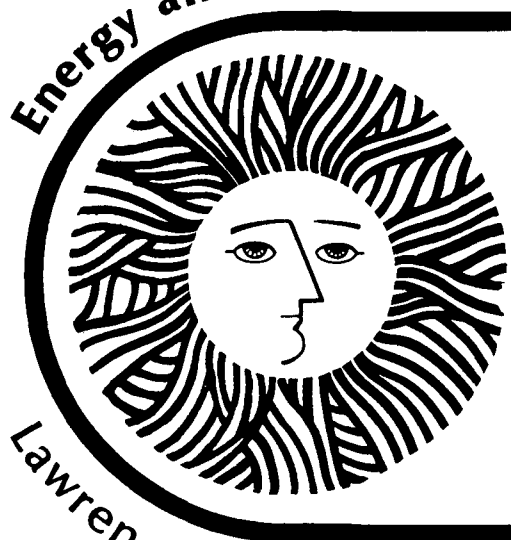
This is a Library Circulating Copy
which may be borrowed for two weeks.
For a personal retention copy, call
Tech. Info. Division, Ext. 6782

RECEIVED
LAWRENCE
BERKELEY LABORATORY

AUG 30 1978

LIBRARY AND
DOCUMENTS SECTION

Energy and Environment Division



Heat Transfer During
Piston Compression

M. Nikanjam and R. Greif

July 1978

Lawrence Berkeley Laboratory University of California/Berkeley

Prepared for the U.S. Department of Energy under Contract No. W-7405-ENG-48
and the National Science Foundation under NSF/RANN Grant AER-76-08727

LBL-7838

c.2

DISCLAIMER

This document was prepared as an account of work sponsored by the United States Government. While this document is believed to contain correct information, neither the United States Government nor any agency thereof, nor the Regents of the University of California, nor any of their employees, makes any warranty, express or implied, or assumes any legal responsibility for the accuracy, completeness, or usefulness of any information, apparatus, product, or process disclosed, or represents that its use would not infringe privately owned rights. Reference herein to any specific commercial product, process, or service by its trade name, trademark, manufacturer, or otherwise, does not necessarily constitute or imply its endorsement, recommendation, or favoring by the United States Government or any agency thereof, or the Regents of the University of California. The views and opinions of authors expressed herein do not necessarily state or reflect those of the United States Government or any agency thereof or the Regents of the University of California.

HEAT TRANSFER DURING PISTON COMPRESSION

M. Nikanjam^{*} and R. Greif

University of California, Berkeley
Department of Mechanical Engineering and
Lawrence Berkeley Laboratory
Berkeley, California 94720

*Present address: Union Carbide Corporation, Bound Brook, New Jersey

ABSTRACT

An experimental and theoretical study has been carried out to determine the unsteady heat transfer from a non-reacting gas to the end wall of a channel during the piston compression of a single stroke. A thin platinum film resistance thermometer records the surface temperature of the wall during the compression. A conduction analysis in the wall, subject to the measured surface temperature variation, then yields the unsteady heat flux. A separate analysis based on the solution of the laminar boundary layer equations in the gas provides an independent determination of the heat flux. The two results are shown to be in good agreement. This is true for measurements that were made in air and in argon. Results for the heat transfer coefficient as a function of time are also presented and exhibit a non-monotonic variation.

INTRODUCTION

The determination of the heat transfer from a gas to an enclosure during piston compression represents a problem that is of considerable practical importance as well as being one of fundamental interest. With respect to internal combustion engines, wall heat transfer processes are critical to the quenching of wall reactions leading to high hydrocarbon emissions, the durability of engine components, the loss of energy leading to decreased efficiency, etc. [1 - 5]. The transient, variable volume (moving surface), variable pressure aspects of the compression process result in complex phenomena that are difficult to appraise (for example, refer to [6 - 9]).

The present experiments were carried out in a single pulse, compression-expansion apparatus [8]. The work is an experimental and theoretical study of the unsteady end wall heat transfer during piston compression. The measurements were carried out during the compression stroke of a single pulse.

EXPERIMENTAL APPARATUS AND MEASUREMENTS

The present set of measurements was carried out to determine the heat transfer from a gas to the wall of a channel of square cross-section during piston compression. The apparatus used was a stainless steel enclosure that was fitted with a pneumatically operated piston (cf. Oppenheim, et al. (8)). There are three main elements in the apparatus; the compression chamber or test section, the driving chamber and the displacement control chamber. The chambers are separated from each other by bearings and seals, and contain separate pistons which are connected by an adjustable shaft (cf. Figure 1).

The test section has four ports on the top and four ports on the bottom walls. The chamber can be purged and filled through these ports which may also be used for temperature and pressure measurements. The end block of the chamber also has a port which may be adjusted to allow for a variety of configurations. The test section, 38 mm x 38 mm, contains an aluminum piston that is fitted with teflon seals. The test piston is connected by an aluminum rod to another piston in the driving chamber. The driving force for this piston is provided by the pressure difference across the piston. The pressure is supplied from compressed gas stored in a large tank near the apparatus. The flow through the driving chamber is controlled by a system of solenoid valves that are operated electronically.

The displacement control chamber is filled with oil and contains a series of snubbers which vary in inside diameter. The controlling piston in this snubber section, which is connected to the driver piston, moves first in an area of increasing cross section, then in a constant area and finally into a region of decreasing cross sectional area. The snubbers can be changed to provide for different trajectories and strokes. A typical stroke for the present experiments was 5 in (130 mm) with a compression ratio of 8 and a time interval of 30 msec.

The main shaft extends beyond the snubber section and is fitted with a steel rack with a set of teeth. Opposite the shaft is a magnetic pickup that senses the teeth as they pass by. The corresponding change in voltage is then recorded as a function of time (cf. Figure 2) which yields the piston displacement as a function of time. To determine the pressure in the test section as a function of time, a Kistler pressure transducer (SN 52036) was placed in one of the ports. The output is shown in Figure 2.

To measure the temperature of the wall as a function of time, a thin-film resistance thermometer was used. This gauge was built to fit the end block, and also the side wall of the test section, and was mounted flush with the wall to avoid disturbing the flow. The resistance thermometer consisted of a thin platinum film on an insulated backing. In the present experiments platinum was painted on a machinable glass-ceramic base (Macor, made by Corning Glass Works). The gauge was then baked in an oven to a temperature of 750°C to drive off the volatile constituents and to obtain a good metal-glass bond. Typically, the films had a resistance of 100 ohms with typical dimensions 1.3 cm x 0.3 cm.

The resistance thermometer was connected as the active element in a D.C. bridge. A temperature change caused a change in resistance of the platinum film which caused an unbalance in the bridge. The resulting voltage was then amplified and displayed on a Tektronix oscilloscope (cf. Figure 2). For calibration purposes the resistance thermometer was placed in an enclosure that was thermally controlled and the voltage output of the bridge was recorded as a function of the temperature. The calibration tests were performed before and after the experiments and no changes were observed.

Numerous studies have been carried out with thin-film resistance thermometers (9-21). These studies have demonstrated the durability of

these gauges and their rapid response times. Indeed, calculations give a response time that is less than one microsecond and this has been confirmed by measurements that were made with these gauges in a shock tube. One important application has been in the determination of the wall heat flux based on the measured surface temperature histories. The evaluation of the heat flux is dependent on the properties of the insulating base, in particular on the parameter $(\rho ck)^{\frac{1}{2}}$. The value of this parameter obtained directly from experimental gauge measurements for a pyrex base (13,16,21) is $0.036 \text{ cal/cm}^2\text{°C sec}^{\frac{1}{2}}$ ($0.151 \text{ watt sec}^{\frac{1}{2}}/\text{cm}^2\text{°K}$) which is in very good agreement with the value calculated from the bulk properties of pyrex; namely, $0.035 \text{ cal/cm}^2\text{°C sec}^{\frac{1}{2}}$ ($0.146 \text{ watt sec}^{\frac{1}{2}}/\text{cm}^2\text{°K}$). The value of $(\rho ck)^{\frac{1}{2}}$ for Macor based on the values of the bulk properties (22) is $0.033 \text{ cal/cm}^2\text{°C sec}^{\frac{1}{2}}$ ($0.138 \text{ watt sec}^{\frac{1}{2}}/\text{cm}^2\text{°K}$) and this is the value that has been used in the present experiments.

ANALYSIS

The determination of the heat flux during piston compression is based on the measured surface temperature of a thermally infinite solid (Macor) that is initially at a constant temperature. The solution for the wall heat flux is given by [16]:

$$q_{w,s} = \left(\frac{k\rho c}{\pi} \right)^{1/2} \int_0^t \frac{1}{(t - \bar{t})^{1/2}} \frac{dT_w}{d\bar{t}} d\bar{t} \quad (1)$$

To perform the numerical calculations for the heat flux it is more convenient to use the following form of Eq. (1) [16]:

$$q_{w,s} = \left(\frac{k\rho c}{\pi} \right)^{1/2} \left\{ \frac{T_w(t) - T_i}{t^{1/2}} + \frac{1}{2} \int_0^t \frac{T_w(t) - T_w(\bar{t})}{(t - \bar{t})^{3/2}} d\bar{t} \right\} \quad (2)$$

which does not involve measurement of slopes.

An alternative approach for the determination of the wall heat flux is based on a solution of the conservation equations in the gas as applied to the thin boundary layer near the end wall. Neglecting viscous dissipation and taking the pressure to be uniform yields the following one-dimensional equations of continuity and energy:

$$\frac{\partial \rho}{\partial t} + \frac{\partial(\rho u)}{\partial x} = 0 \quad (3)$$

$$\rho c_p \left[\frac{\partial T}{\partial t} + \frac{u \partial T}{\partial x} \right] = \frac{dp_\infty}{dt} + \frac{\partial}{\partial x} \left(k \frac{\partial T}{\partial x} \right) \quad (4)$$

where x is the coordinate perpendicular to the wall. These are the same equations used by Isshiki and Nishiwaki (20) in their study of the effects of cyclic changes in an internal combustion engine and their analysis is used below. (For the simpler constant pressure problem refer to (18)). The continuity equation is satisfied by a stream coordinate ψ according to

$$\frac{\rho}{\rho_i} = \frac{\partial \psi}{\partial x}, \quad \frac{\rho u}{\rho_i} = - \frac{\partial \psi}{\partial t} \quad (5)$$

where ρ_i is the initial density (or a density at a specified state) of the gas. Using the ideal gas law, $p_\infty = \rho RT$ and a linear thermal conductivity variation with respect to temperature, the energy equation becomes in ψ, t coordinates:

$$\frac{\partial T}{\partial t} = \frac{\gamma-1}{\gamma} \frac{T}{p_\infty} \frac{dp_\infty}{dt} + \alpha_i \frac{p_\infty}{p_i} \frac{\partial^2 T}{\partial \psi^2} \quad (6)$$

The transformation $d\tau = (p_\infty/p_i)dt$ (20) then yields

$$\frac{\partial T}{\partial \tau} = \frac{\gamma-1}{\gamma} \frac{T}{p_\infty} \frac{dp_\infty}{d\tau} + \alpha_i \frac{\partial^2 T}{\partial \psi^2} \quad (7)$$

The gas outside the boundary layer is assumed to be compressed isentropically so that $p_\infty/p_i = (T_\infty/T_i)^{\gamma/(\gamma-1)}$. Making this substitution yields

$$\frac{\partial T}{\partial \tau} = \frac{T}{T_\infty} \frac{dT_\infty}{d\tau} + \alpha_i \frac{\partial^2 T}{\partial \psi^2} \quad (8)$$

Then, introducing the variable $\phi = T/T_\infty$ into Eq. (8) gives (20)

$$\frac{\partial \phi}{\partial \tau} = \alpha_i \frac{\partial^2 \phi}{\partial \psi^2} \quad (9)$$

subject to the conditions

$$\phi(\psi, 0) = 1$$

$$\phi(0, \tau) = T_w/T_\infty = T_w/T_i (V_i/V)^{\gamma-1} = \phi_w \quad (10)$$

$$\phi(\infty, \tau) = 1$$

Note that the wall location corresponds to $\psi = 0$.

The solution for the wall heat flux is then given by (16):

$$q_{w,g} = +k_w \left. \frac{\partial T}{\partial x} \right|_{x=0} = - \frac{k_w \rho_w T_\infty}{\rho_i (\pi \alpha_i)^{1/2}} \int_0^\tau \frac{1}{(\tau - \bar{\tau})^{1/2}} \frac{d\phi_w}{d\bar{\tau}} d\bar{\tau} \quad (11)$$

or

$$q_{w,g} = - \frac{k_w \rho_w T_\infty}{\rho_i (\pi \alpha_i)^{1/2}} \left\{ \frac{\phi_w(\tau) - 1}{\tau^{1/2}} + \frac{1}{2} \int_0^\tau \frac{\phi_w(\tau) - \phi_w(\bar{\tau})}{(\tau - \bar{\tau})^{3/2}} d\bar{\tau} \right\} \quad (12)$$

RESULTS AND DISCUSSION

Experiments were carried out in air and in argon with the thin film gauge placed at the end wall of the compression chamber. Typical results for the unsteady heat flux as determined from both the solution of the conduction equation in the solid, $q_{w,s}$, and from the solution of the laminar boundary layer conservation equations in the gas, $q_{w,g}$, are presented in Figures 3 and 4. The results for the heat flux from these two independent methods are seen to be in good agreement although we do have more confidence in the result based on the conduction analysis in the solid. This is because the calculation for $q_{w,s}$ only depends on the variation of the wall temperature, T_w , and the constant properties of the solid. In contrast, the calculation for $q_{w,g}$ requires the specification of: the variation of the thermal conductivity of the gas with respect to temperature; the piston trajectory, that is, the volume of the compressed gas as a function of time; etc. It is noted that the determination of $q_{w,s}$ is influenced by the value of the parameter $(\rho ck)^{1/2}$, the non-zero thickness of the platinum film and the sensitivity of the gauge. On the basis of numerous investigations it has been concluded that the heat flux can be determined to an accuracy from ± 5 to ± 15 percent [16].

In the determination of the heat flux $q_{w,g}$, the dependent variable was shown to be $\phi_w = T_w/T_\infty = T_w/T_i (V_i/V)^{\gamma-1}$. Calculations were carried out for constant and for time varying values of the wall temperature, but because the variation in the wall temperature was small in comparison to the much larger variation of T_∞ , the results were essentially the same. There are many applications when the variation in T_w is small

and is not measured (so that the conduction analysis in the solid cannot then be used as the basis for determining the heat flux). Hence, for these applications $q_{w,g}$ (which is in good agreement with $q_{w,s}$) provides the basis for calculating the heat flux. In detail, for $\phi_w(\tau) = T_w(\tau)/T_\infty(\tau) \approx \text{constant}/T_\infty(\tau)$, Eq. (12) becomes

$$q_{w,g} = \frac{-k_w \rho_w}{\rho_i (\pi \alpha_i)^{1/2}} \left\{ \frac{T_w - T_\infty(\tau)}{\tau^{1/2}} + \frac{T_\infty(\tau) T_w}{2} \int_0^\tau \frac{T_\infty^{-1}(\tau) - T_\infty^{-1}(\bar{\tau})}{(\tau - \bar{\tau})^{3/2}} d\bar{\tau} \right\} \quad (13)$$

so that the heat flux is determined solely from the variation of T_∞ .

Of particular interest is the result for the heat transfer coefficient during piston compression which is obtained from the relation

$$h = \frac{q_{w,s}}{T_\infty - T_w} = \frac{1}{T_\infty(t) - T_w(t)} \left(\frac{k \rho c}{\pi} \right)^{1/2} \left\{ \frac{T_w(t) - T_i}{t^{1/2}} + \frac{1}{2} \int_0^t \frac{T_w(t) - T_w(\bar{t})}{(t - \bar{t})^{3/2}} d\bar{t} \right\} \quad (14)$$

The results for h are presented in Figures 5 and 6 along with the values for V/V_i , T_∞ , T_w and $q_{w,s}$. The values for h based on $q_{w,g}$ are in good agreement with those based on $q_{w,s}$ and are therefore not shown. Note that the heat transfer coefficient first decreases with time but as the compression continues, h reaches a minimum value and then increases with time. At the beginning of the compression the increase in the boundary layer thickness with time causes the heat transfer coefficient to decrease. However, as the compression continues the convective transport (in the boundary layer towards the wall) becomes more important, finally causing the heat transfer coefficient to increase as shown in Figures 5 and 6. This convective transport

is a result of the drop in the gas temperature between the outer region and the region near the wall and the associated increase in density near the wall. Indeed, the density increase is brought about by the convection of the gas towards the wall. Reference to [18] should also be made which considers this effect in respect to a constant pressure problem.

It is noted that under ideal conditions the piston should come to a smooth stop at the end of the compression stroke. However, in practice the piston rebounds near the end of the stroke. This is accompanied by a decrease in the pressure which is followed by a slight rise as the piston completes the compression and then comes to the final position (cf. Fig. 2).

In closing it is pointed out that there is some effect due to mixing in the gas resulting from the vortex that forms at the piston-wall interface [6 - 8]. This effect is directly reflected in the result for the heat flux from the conduction analysis in the solid via the measured wall temperature variation. However, in the boundary layer conservation equations in the gas any mixing effect must also be included as an additional convective transport mechanism. The omission of this contribution is consistent with the slightly smaller results obtained for $q_{w,g}$ in comparison to $q_{w,s}$. Furthermore, the velocity of the piston directly imparts a velocity to the gas which has also been omitted in the boundary layer analysis. This is (also) consistent with the slightly smaller results for $q_{w,g}$.

CONCLUSIONS

The unsteady wall heat flux during piston compression of a single stroke has been determined by two independent methods. The heat transfer based on the laminar boundary layer equations and the piston trajectory yields results that are in good agreement with the flux obtained from the conduction analysis in the solid. This is true for end wall measurements that were made in air and in argon. Results for the heat transfer coefficient for all cases exhibit a non-monotonic variation with respect to time.

ACKNOWLEDGMENT

The authors acknowledge with appreciation the support of this research by the National Science Foundation under NSF/RANN Grant AER-76-08727 and by the U.S. Energy Research and Development Administration under Contract W-7405-ENG-48.

1. Overbye, V.D., Bennethum, J.E., Uyehara, O.A., and Myers, P.S., "Unsteady heat transfer in engines", Society of Automotive Engineers Transactions, Vol. 69, 1961, pp. 461-494.
2. Annand, W.J.D., "Heat transfer in the cylinders of reciprocating internal combustion engines", Proc. I. Mech. E., Vol. 177, 1963, pp. 973-996.
3. LeFeuvre, T., Myers, P.S., and Uyehara, O.A., "Experimental instantaneous heat fluxes in a diesel engine and their correlation", Society of Automotive Engineers Transactions, Vol. 78, 1969, 690464, pp.1717-1738.
4. Dao, K., Uyehara, O.A., and Myers, P.S., "Heat transfer rates at gas-wall interfaces in motored piston engines", Society of Automotive Engineers Transactions, Vol. 82, 730632, 1974, pp. 2237-2258.
5. Chong, M.S., Milkins, E.E., and Watson, H.C., "The prediction of heat and mass transfer during compression and expansion in I.C. engines", Society of Automotive Engineers, 760761, 1976.
6. Tabaczynski, R.J., Hoult, D.P., and Keck, J.C., "High Reynolds Number Flow in a Moving Corner", J. Fluid Mech., Vol. 42, 1970, pp. 249-256.
7. Daneshyar, H., Fuller, D.E., and Decker, B.E.L., "Vortex motion induced by the piston of an internal combustion engine", Int. J. Mech. Sci., Vol. 15, 1973, pp. 381-390.
8. Oppenheim, A.K., Chang, R.K., Teichman, K., Smith, O.I., Sawyer, R.F., Ham, K., and Stewart, H.E., "A cinematographic study of combustion in an enclosure filled with a reciprocating piston", Conference on Stratified Charge Engines, London, England, 1976.
9. Witze, P.O., "Hot-wire measurements of the turbulent structure in a motored spark-ignition engine", AIAA Paper No. 76-37, 1976.
10. Pfried, H., "Zur messung schnell wechselnder temperatures in des zylinderwand von kolbenmaschinen", Forschung Ing.-West., Bd. 6, Heft 4, 1935, pp. 195-201.
11. Meier, A., "Recording rapidly changing cylinder-wall temperatures", translation, NACA TM 1013, 1939.
12. Rabinowicz, J., Jessey, M.E., and Bartsch, C.A., "Resistance thermometer for heat transfer measurement in a shock tube", GALCIT Hypersonic Research Project Memo, 33, Guggenheim Aeronautical Laboratory, California Institute of Technology, July 1956.
13. Vidal, R., "Model instrumentation techniques for heat transfer and force measurements in a hypersonic shock tunnel", Report AD 917-A-1, Buffalo, N.Y., Cornell Aeronautical Laboratory, Inc., 1956.
14. Bromberg, R., "Use of the shock tube wall boundary layer in heat transfer studies", Jet Propulsion, Vol. 26, September 1956, pp. 737-740.
15. Rose, P.H., and Stark, W.I., "Stagnation point heat transfer measurements in air at high temperature", Research Note 24, Everett, Mass., AVCO Research Laboratory, AVCO Manufacturing Corp., December 1956.

16. Hall, J.G. and Hertzberg, A., "Recent advances in transient surface temperature thermometry," *Jet Propulsion*, Vol. 28, 1958, pp. 719-723.
17. Bogdan, L., "High-temperature, thin-film resistance thermometers for heat transfer measurement," *NASA Contractor Report*, NASA CR-26, April 1964.
18. Collins, D.J., Greif, R. and Bryson, A.E., "Measurements of the thermal conductivity of helium in the temperature range 1600-6700°K," *Int. J. Heat Mass Transfer*, Vol. 8, 1965, pp. 1209-1216.
19. Collins, D.J., "Shock tube study for the determination of the thermal conductivity of neon, argon and krypton," *J. Heat Transfer*, Trans. ASME, Series C, Vol. 88, 1966, pp. 52-56.
20. Isshiki, N. and Nishiwaki, N., "Study on laminar heat transfer of inside gas with cyclic pressure change on an inner wall of a cylinder head," *4th International Heat Transfer Conference*, Paris-Versailles, 1970, FC 3.5, pp. 1-10.
21. Skinner, G.T., "Calibration of the thin-film gauge backing materials," *ARS J.*, Vol. 31, 1961.
22. Grossman, D.G., *Corning Glass Works*, personal communication; also, Pamphlet MGS 274-2.

NOMENCLATURE

c	=	specific heat of solid
c_p	=	specific heat of gas
h	=	heat transfer coefficient
k	=	thermal conductivity
p	=	gas pressure
q	=	heat flux
R	=	gas constant
t	=	time
T	=	temperature
u	=	gas velocity
V	=	volume
x	=	coordinate normal to wall
α	=	$k/\rho c_p$ thermal diffusivity
γ	=	ratio of the specific heats
ϕ	=	$\frac{T}{T_\infty}$ = temperature ratio
ρ	=	density
ψ	=	stream coordinate
τ	=	transformed time

Subscripts

g	=	gas
i	=	initial
s	=	solid
w	=	wall
∞	=	outside boundary layer

LIST OF FIGURES

Figure 1 Experimental apparatus including (A) compression chamber, (B) driving chamber and (C) displacement control chamber.

Figure 2 Typical oscillogram for surface temperature, displacement and pressure measurements.

Figure 3 Heat flux variation.

Figure 4 Heat flux variation.

Figure 5 Measured and calculated variables.

Figure 6 Measured and calculated variables.

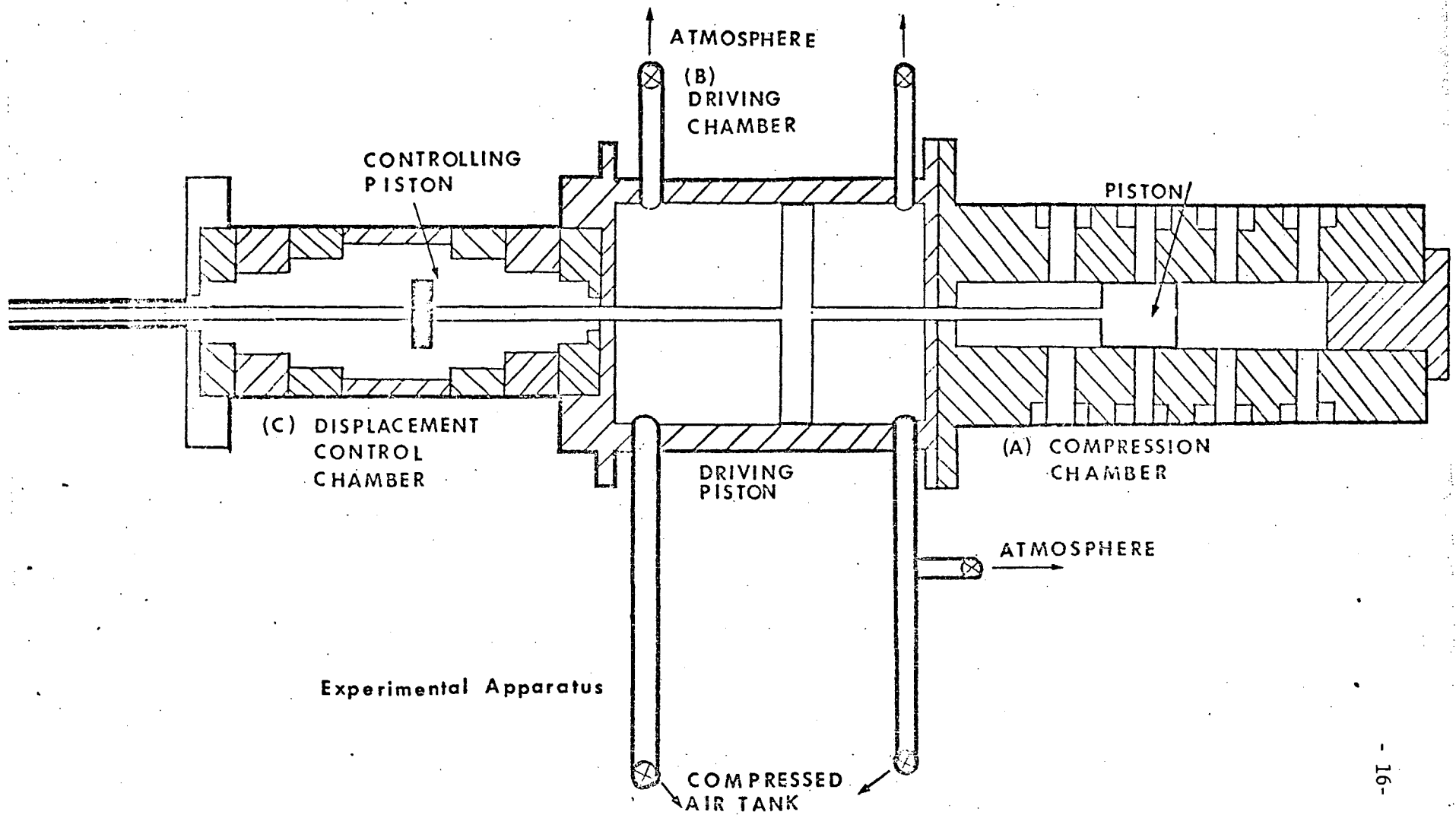
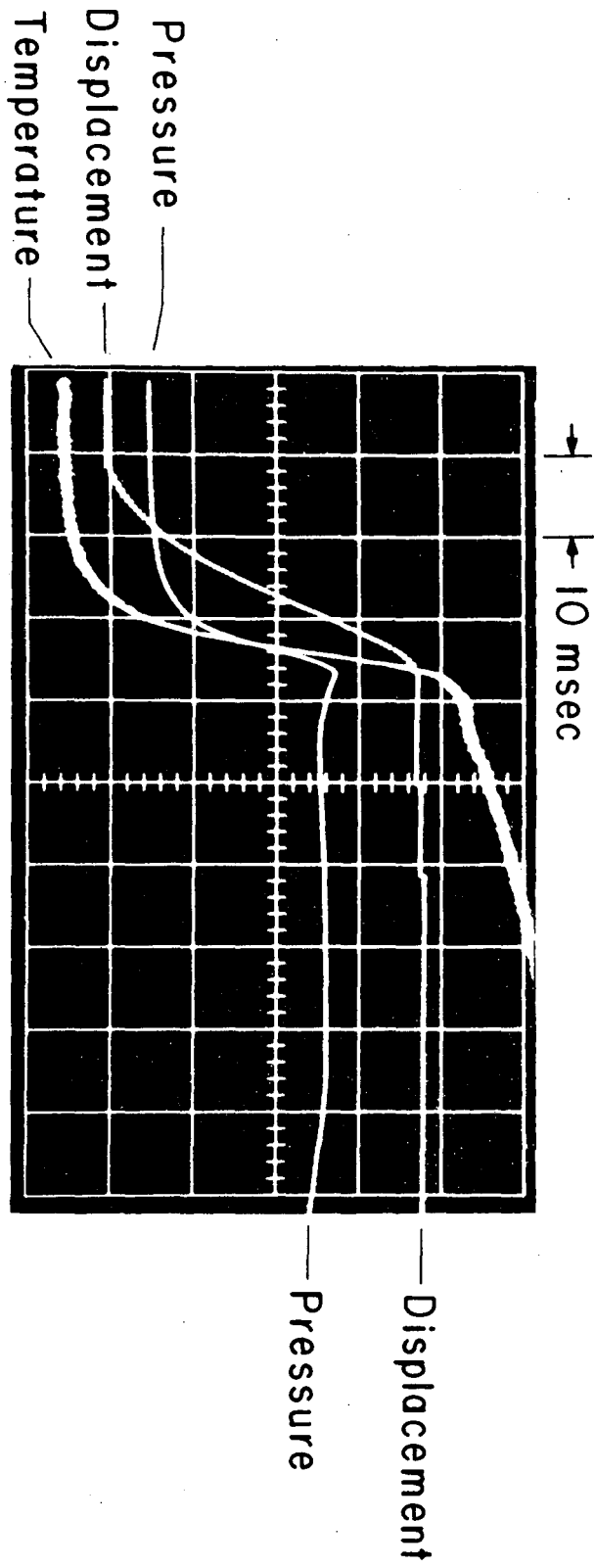


Figure 1 Experimental apparatus including (A) compression chamber, (B) driving chamber and (C) displacement control chamber.



XBL 786-9438

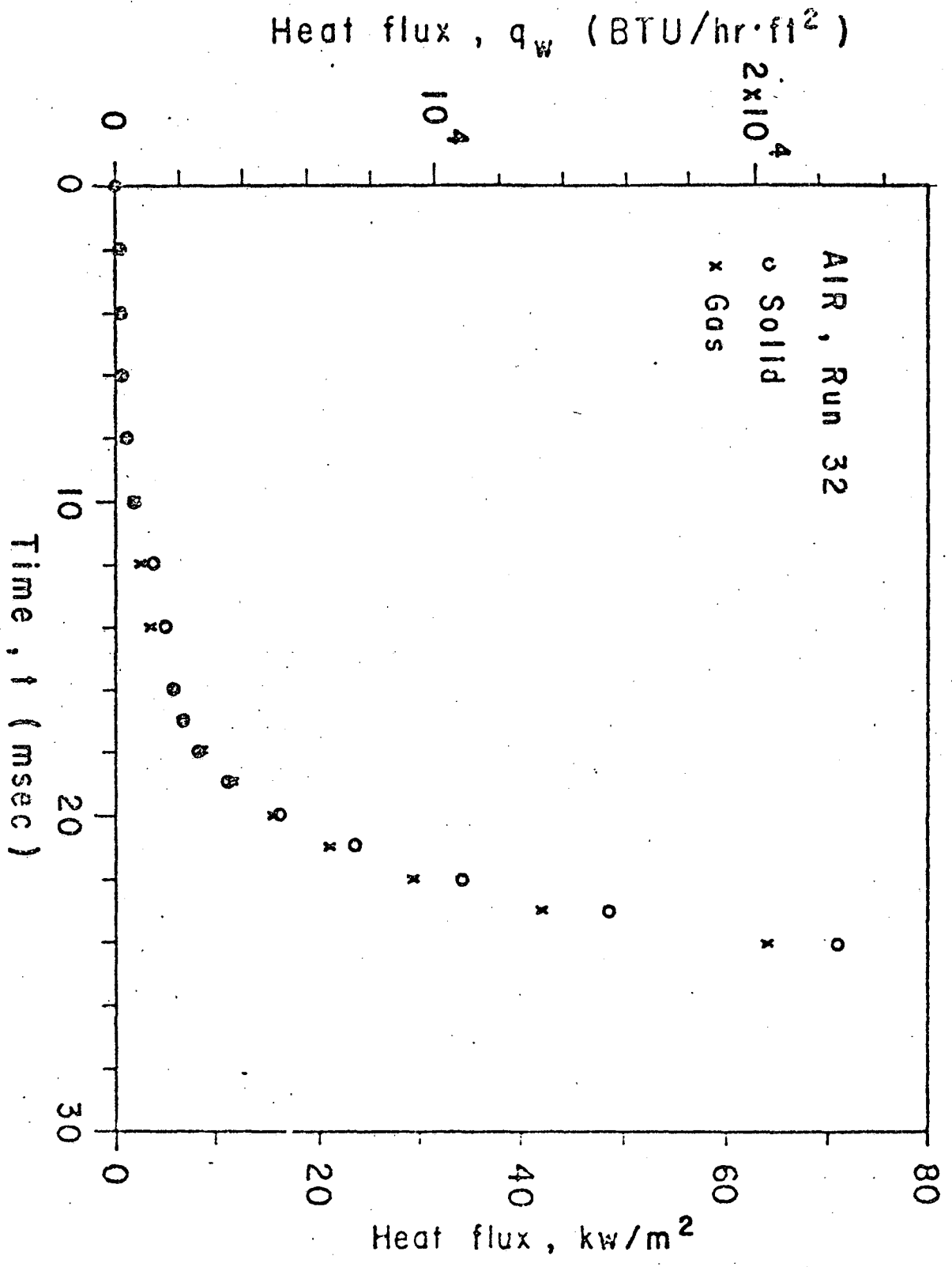


Figure 3 Heat flux variation.

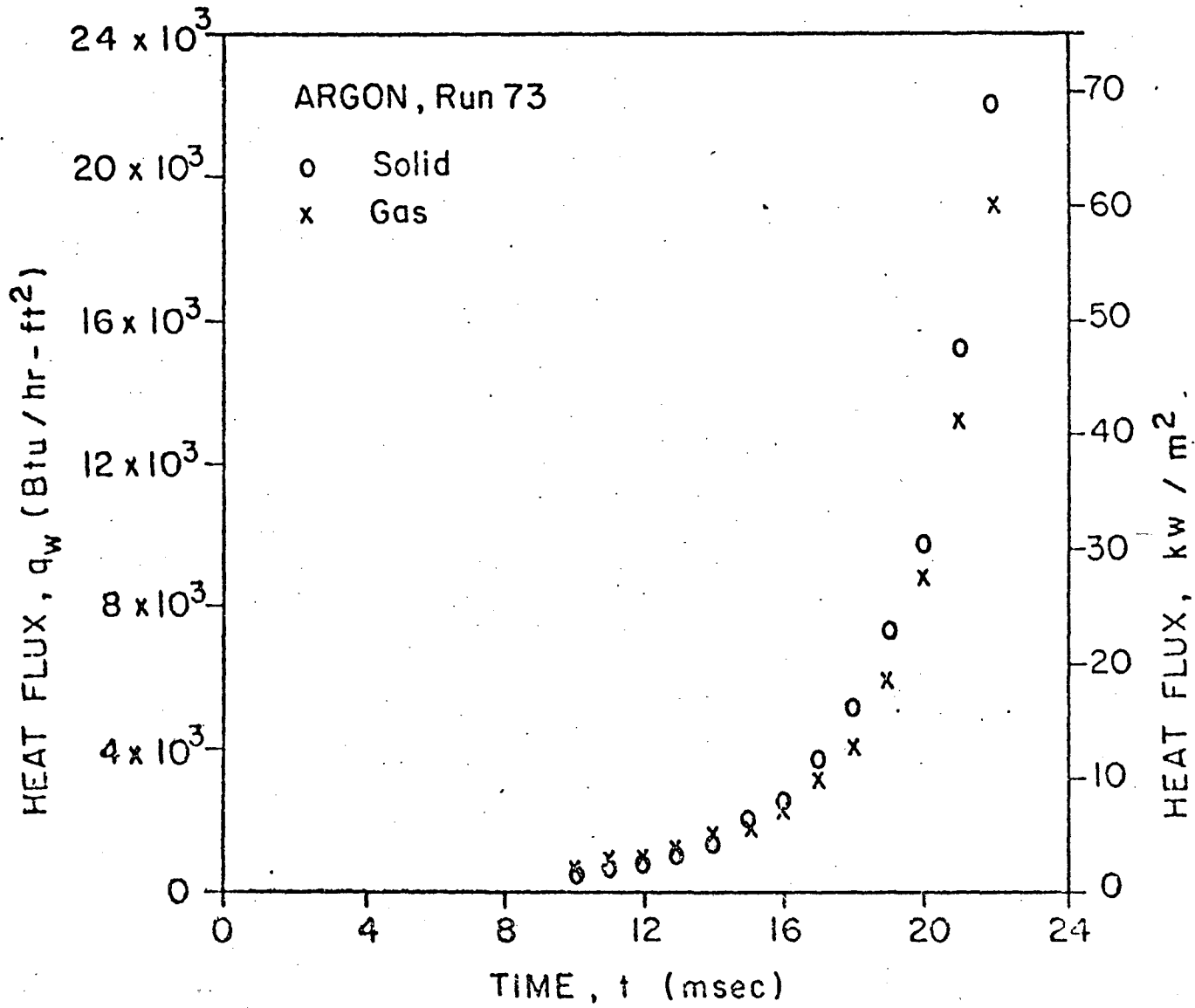


Figure 4 Heat flux variation.

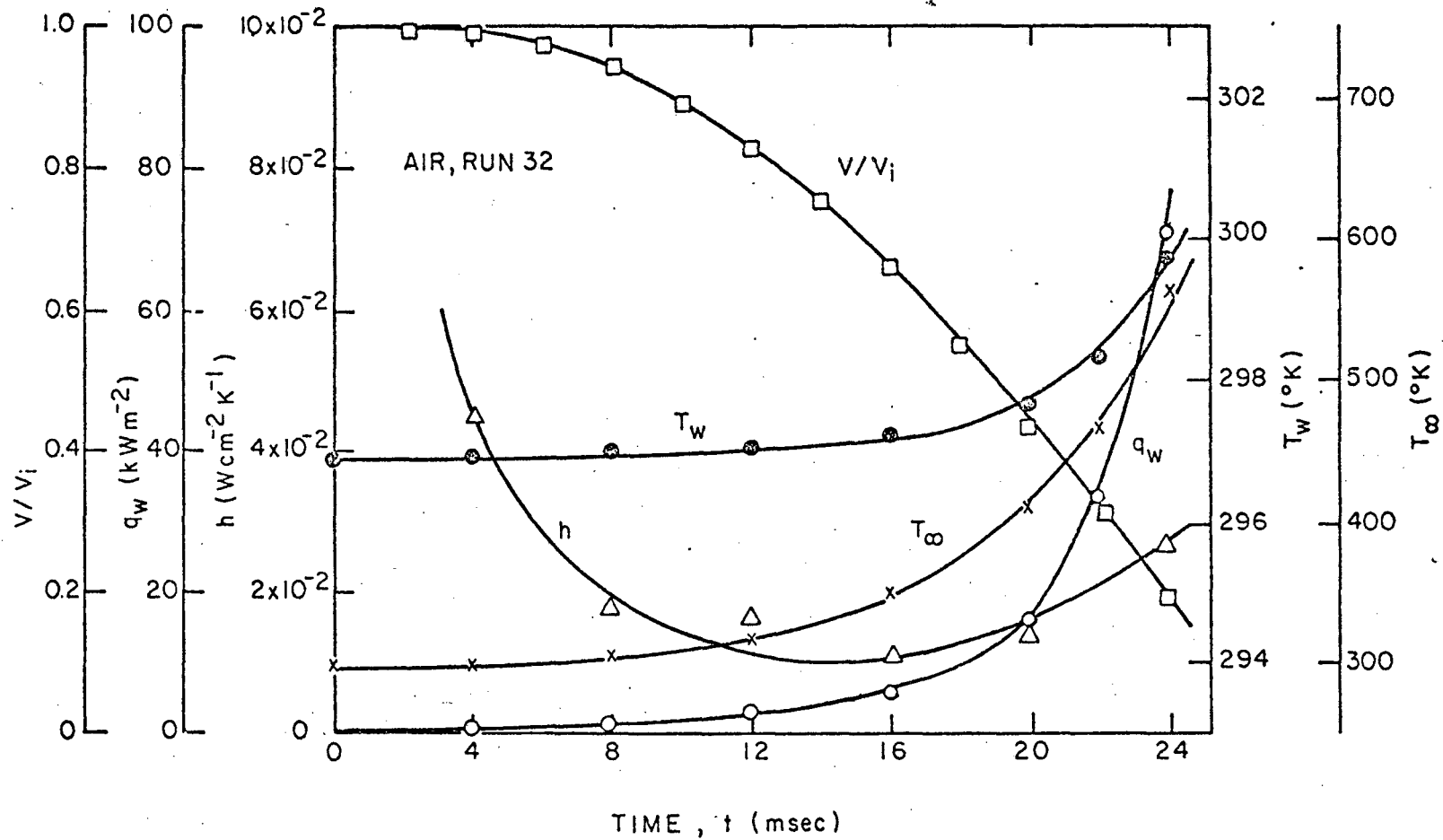


Figure 5 Measured and calculated variables.

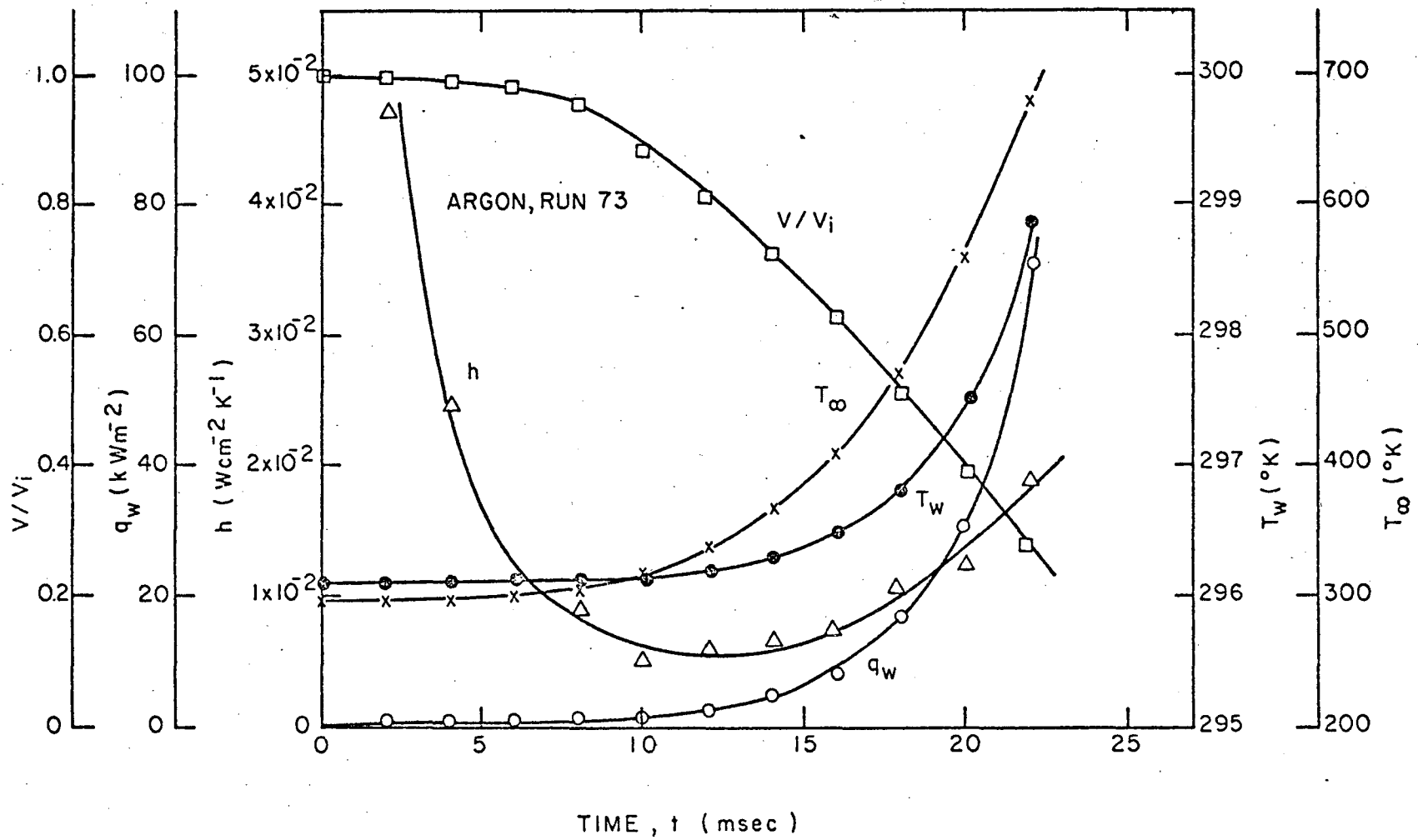


Figure 6 Measured and calculated variables.

This report was done with support from the Department of Energy. Any conclusions or opinions expressed in this report represent solely those of the author(s) and not necessarily those of The Regents of the University of California, the Lawrence Berkeley Laboratory or the Department of Energy.

TECHNICAL INFORMATION DEPARTMENT
LAWRENCE BERKELEY LABORATORY
UNIVERSITY OF CALIFORNIA
BERKELEY, CALIFORNIA 94720